

## Video Article

# Construction and Characterization of a Novel Vocal Fold Bioreactor

Aidan B. Zerdoum<sup>1</sup>, Zhixiang Tong<sup>2</sup>, Brendan Bachman<sup>2</sup>, Xinqiao Jia<sup>1,2</sup><sup>1</sup>Biomedical Engineering Program, University of Delaware<sup>2</sup>Department of Materials Science and Engineering, Delaware Biotechnology Institute, University of DelawareCorrespondence to: Xinqiao Jia at [xjia@udel.edu](mailto:xjia@udel.edu)URL: <http://www.jove.com/video/51594>DOI: [doi:10.3791/51594](https://doi.org/10.3791/51594)

Keywords: Bioengineering, Issue 90, vocal fold; bioreactor; speaker; silicone membrane; fibrous scaffold; mesenchymal stem cells; vibration; extracellular matrix

Date Published: 8/1/2014

Citation: Zerdoum, A.B., Tong, Z., Bachman, B., Jia, X. Construction and Characterization of a Novel Vocal Fold Bioreactor. *J. Vis. Exp.* (90), e51594, doi:10.3791/51594 (2014).

## Abstract

*In vitro* engineering of mechanically active tissues requires the presentation of physiologically relevant mechanical conditions to cultured cells. To emulate the dynamic environment of vocal folds, a novel vocal fold bioreactor capable of producing vibratory stimulations at fundamental phonation frequencies is constructed and characterized. The device is composed of a function generator, a power amplifier, a speaker selector and parallel vibration chambers. Individual vibration chambers are created by sandwiching a custom-made silicone membrane between a pair of acrylic blocks. The silicone membrane not only serves as the bottom of the chamber but also provides a mechanism for securing the cell-laden scaffold. Vibration signals, generated by a speaker mounted underneath the bottom acrylic block, are transmitted to the membrane aerodynamically by the oscillating air. Eight identical vibration modules, fixed on two stationary metal bars, are housed in an anti-humidity chamber for long-term operation in a cell culture incubator. The vibration characteristics of the vocal fold bioreactor are analyzed non-destructively using a Laser Doppler Vibrometer (LDV). The utility of the dynamic culture device is demonstrated by culturing cellular constructs in the presence of 200-Hz sinusoidal vibrations with a mid-membrane displacement of 40  $\mu\text{m}$ . Mesenchymal stem cells cultured in the bioreactor respond to the vibratory signals by altering the synthesis and degradation of vocal fold-relevant, extracellular matrix components. The novel bioreactor system presented herein offers an excellent *in vitro* platform for studying vibration-induced mechanotransduction and for the engineering of functional vocal fold tissues.

## Video Link

The video component of this article can be found at <http://www.jove.com/video/51594/>

## Introduction

The human vocal fold, composed of an epithelial layer, the lamina propria (LP) and the vocalis muscle, is a specialized soft tissue that converts air flow from the lungs into acoustic waves for sound production.<sup>1</sup> Vocal folds oscillate regularly during normal phonation, exhibiting strains of up to 30% at fundamental frequencies ranging from 100-300 Hz.<sup>2</sup> Adult vocal fold LP is a gradient structure composed of a superficial (SLP), an intermediate (ILP) and a deep (DLP) layer. Further classification groups the epithelium and the SLP as the mucosa layer, and combines the ILP and DLP into the vocal ligament.<sup>3</sup> The SLP layer contains primarily an amorphous matrix with sparsely dispersed collagenous fibers, while the ligament is enriched with mature collagen and elastin fibers to provide sufficient strength.<sup>4</sup> The structure and mechanics of newborn vocal folds vary significantly from their mature counterparts. Although mechanisms regulating vocal fold development and maturation are not yet fully understood, experimental evidence has pointed to the defining roles of vocalization-derived mechanical stress.

Several medical conditions, including voice abuse, infections, chemical irritants and surgical procedures, can damage the vocal fold. Vocal fold disorders affect an estimated 3-9% of the U.S. population. Current treatment methods for vocal fold disorders are limited<sup>5</sup> and a stem cell-based tissue engineering approach has emerged as a promising strategy for restoring vocal fold function. Mesenchymal stem cells (MSCs) are a suitable alternative to the primary vocal fold fibroblasts for vocal fold tissue engineering.<sup>6-9</sup> Stem cell fate specification and subsequent tissue development are mediated by the specific niche they reside in, of which the mechanical condition is a vital factor.<sup>10</sup> Mechanical forces are essential regulators of tissue morphogenesis and homeostasis, especially for tissues that are routinely subjected to loading.<sup>11</sup> From a tissue engineering perspective, it has been demonstrated that exposure to physiologically relevant mechanical stimulations promotes stem cell differentiation and tissue-specific matrix remodeling.<sup>12-15</sup>

Tissue culture bioreactors are designed to simulate the desired physiological environment for cell or tissue growth *in vitro*. For vocal fold tissue engineering, it is especially critical to recreate the mechanical environment of the phonating vocal folds. An ideal vocal fold bioreactor should effectively deliver vibratory cues to culture cells, allowing facile control over frequency, amplitude and duration of vibrations. Titze and coworkers devised a vocal fold bioreactor (*T1 bioreactor*)<sup>16</sup> that combines static stretch with high frequency (20-200 Hz) oscillations to stimulate the cellular production of matrix proteins. Using this bioreactor, Webb and colleagues<sup>17</sup> studied the effects of 10-day, 100-Hz vibrations on dermal fibroblasts cultured in a hyaluronic acid (HA)-based hydrogel. Constructs subjected to vibration exhibited an elevated expression of HA synthase-2 (HAS2), decorin, fibromodulin and matrix metalloproteinase-1 (MMP1), relative to the static controls. The stimulatory effects were found to be time dependent. More recently, our group<sup>18</sup> assembled a vocal fold bioreactor (*J1 bioreactor*) using a power amplifier, a function generator, an

enclosed loud speaker and a circumferentially-anchored silicone membrane that transfers the oscillating air to the attached cells. Neonatal foreskin fibroblasts cultivated in the *J1* bioreactor were subjected to 1 hr of vibration at 60, 110 or 300 Hz, with an in-plane strain of up to 0.05%. The qPCR results suggested that the expression of some ECM genes was moderately altered in response to the varied vibratory frequencies and amplitudes.

These bioreactor designs, while intriguing, have several limitations. For example, the *T1* system requires a large number of connectors and bars for mechanical coupling, limiting the maximum frequencies attainable. Moreover, cells may be subjected to undesirable mechanical agitation and fluid perturbation that complicate the data interpretation. The *J1* bioreactor, on the other hand, exhibits relatively low energy conversion efficiency and is not user-friendly. In addition, vibration frequently detaches the cell-laden constructs from the underlying silicone membrane. The *J2* vocal fold bioreactor reported here, designed based on the same principle as the *J1* version, is optimized for consistency and reproducibility. The phonation-mimicking vibrations are generated aerodynamically in individually fitted vibration chambers where MSC-populated fibrous poly( $\epsilon$ -caprolactone) (PCL) scaffolds are effectively secured. Laser Doppler Vibrometry (LDV) allows the user to verify the vibratory profile of the membrane/scaffold assembly. In our demonstration, MSCs are exposed to 200-Hz sinusoidal vibrations with a 1-hr-on-1-hr-off (OF) pattern for a total of 12 hr daily for 7 days. Cellular responses to the imposed vibratory cues are investigated systematically. Overall, the *J2* vocal fold provides the most user-friendly features, allowing dynamic cell culture studies to be conducted in a high throughput and reproducible fashion.

## Protocol

### 1. Bioreactor Assembly (Video 1)

1. Make an aluminum mold (circular die + spacer pin) with pre-determined inner and outer dimensions (**Figure 1**).
2. Using the mold from step 1.1, fabricate a silicone membrane (diameter: 42 mm, thickness: 1.5 mm, **Figure 1**) with an entrenched sleeve (diameter: 12 mm, thickness ~0.25 mm, shaped by the spacer pin in **Figure 1**) in the middle using a commercially available silicone elastomer kit.
3. Make a pair of acrylic blocks (**Figure 2** (4, 5)) with a circular opening (diameter: 24 mm) in the middle, engrave the top (1.8 cm thick) and bottom (0.9 cm thick) blocks with matching ridges and grooves.<sup>10</sup>
4. Sandwich the silicone membrane between the paired acrylic blocks. Secure the assembly with four corner screws using a micro torque screwdriver set to a constant force (35 cN·m). As a result, a water-tight, 24 mm wide and 18 mm deep vibration chamber is created (**Figure 2C**).
5. Mount a 3" extended range mini-woofer (**Figure 2D**, 8  $\Omega$ /20 W) underneath the vibration chamber through another set of corner screws on the bottom acrylic block. At this point, an individual vibration module is assembled.
6. Replicate seven additional vibration modules. Affix four of them to one of two stationary aluminum bars (40 cm x 10 cm x 2.5 cm) by placing the speaker bases in evenly spaced circular holes (diameter: 7 cm, thickness: 2 cm) cut into the bars. Stabilize each speaker by inserting a screw through the side of the aluminum bar into each circular hole.
7. Individually control the speakers by a speaker selector. Connect individual speakers to the selector by attaching wires to the positive and negative inputs on the speaker body then to the corresponding outputs on the selector. The speaker selector allows the signal from the function generator, after passing through a power amplifier, to reach all eight speakers at once (**Figure 2E**).
8. Place the two chamber arrays, the speaker selector and associated electronics in an anti-humidity enclosure. House the entire assembly in a commercial cell culture incubator.
9. Feed the main cables (through a medical grade PVC tubing) connecting the power amplifier and speaker selector through the filter assembly at the back of the incubator.

### 2. Scaffold Fabrication and Characterization

1. Dissolve PCL pellets in chloroform at a concentration of 15 wt%. Load the solution into a 10 ml syringe capped with a 21 G blunt-ended needle.
2. Lock the syringe onto a programmable syringe pump and set the flow rate at 1 ml/hr.
3. Place the aluminum foil-covered collector across from the needle horizontally, with a needle tip-to-collector distance of ~18 cm.
4. Clamp the positive alligator clip to the middle of the needle, and the ground alligator clip to the aluminum collector, then set the voltage on the high voltage power supply at 15 kV. CAUTION: high voltage, keep distance from the needle.
5. Sequentially turn on the syringe pump and power supply; quickly clean/remove the residual polymer solution surrounding the tip of the needle using a dry paper towel before stable fiber jets and Taylor cone<sup>19</sup> are formed.
6. Allow the fibers to accumulate on the Al collector to a thickness of ~250-300  $\mu$ m (~7 hr under the current spinning conditions). Store the resultant scaffolds in a vacuum desiccator for 1-2 days to remove any residual solvent.
7. Image the scaffolds, sputter coated with gold, using a Scanning Electron Microscope to show consistent fiber morphology.<sup>10</sup>

### 3. Bioreactor Assembly and Characterization

1. Punch a cylindrical disk (diameter: 8 mm) with four arms (length: 2 mm) out of the as-spun PCL mat (**Figure 2A**) by first using a 12 mm diameter biopsy punch to cut the outer diameter of the disk. Then use a second, 8 mm biopsy punch to make four 2 mm long notches evenly spaced around the circular blade to score where the arms are to be cut. After scoring with the 8 mm punch, use a scalpel blade to cut the edges of the arms outward. Insert the scaffold into the groove of the silicone membrane *via* the extended arms (Video 1). Flatten the inserted scaffold by gently pressing the surface using flathead tweezers.
2. Attach a small piece of thin Al foil (8 mm x 2 mm, orthogonal shape, **Figure 2B**) to the PCL scaffold to aid laser reflection.
3. Secure the assembled silicone membrane/PCL scaffold (as detailed in step 1.4) in the vibration chamber. Add 1.5 ml water in the chamber in order to hydrate the PCL scaffold before vibration.

- Using the function generator, introduce vibration signals (e.g., 200 Hz sinusoidal waves with a peak-to-peak voltage,  $V_{pp}$ , of 0.1 V) to the sandwiched acrylic chamber. Use a voltmeter to accurately measure the voltage at each speaker input. Note: the  $V_{pp}$  readout from the function generator will differ from the eventual voltage delivered to the speaker.
- Assemble the single-point LDV and secure the fiber-optic laser sensor head to a pan-tilt head tripod. Angle the sensor head so that it is pointing perpendicular to the tabletop. Connect the LDV sensor head to the data acquisition module via coaxial cable then the module to the laptop via USB.
- Focus the laser beam perpendicularly at various predetermined points on the silicone membrane (**Figure 2B** and **Figure 3**).
- Using the data acquisition software, record the mid-membrane displacement. Click "Acquisition Settings" from the "Options" menu; then change the measurement mode to "FFT". Next, click the "Continuous Measurement" in the main toolbar then click the peak that forms at the chosen frequency (**Figure 6D**) to record displacement.
- Plot the normal mid-membrane displacement ( $w_0$ ) as a function of the relative position across the substrate. Construct a 3D colormap of the surface vibratory profile using Origin 8.5 data analysis software.

## 4. Vibratory Cell Culture

- Sub-culture human bone marrow-derived MSCs in T150 tissue culture flasks at an initial seeding density of 4,000-5,000 cells/cm<sup>2</sup> in MSC maintenance media.
- After 7-8 days of cell culture (to ~85% confluency), trypsinize the cells with a cell dissociation reagent such as accutase, count using a hemocytometer, centrifuge (440 x g for 5 min), and re-suspend the cell pellet in fresh MSC maintenance media at a concentration of  $4.5 \times 10^6$  cells/ml.
- Immerse the PCL scaffold in 70% ethanol O/N. After the solvent is evaporated, expose both sides of the scaffold to germicidal UV light (254 nm) for 5-8 min.
- Soak the PCL scaffold in a 20 µg/ml fibronectin solution at 37 °C for 1 hr. Insert the fibronectin-coated scaffold into the silicone membrane. Assemble the bioreactor as detailed in step 1.
- Distribute 40 µl of the cell suspension evenly on the secured PCL scaffold. Allow the cells to attach for 1-1.5 hr before adding an additional 1.5 ml fresh media to the vibration chamber.
- Culture the MSC-laden PCL scaffold statically for 3 days and refresh the media upon completion of the static culture.
- Impose selected vibration regimes to the cellular constructs. Note: As an example, cells are subjected to a 1-hr-on-1-hr-off (OF) vibration at 200 Hz with a  $w_0$  of ~40 µm for 12 hr per day for up to 7 days. Constructs subjected to vibratory stimulations are designated as Vib samples and those cultured statically in identical vibration chambers serve as static controls (Stat).

## 5. Biological Evaluations

- Collect 200 µl cell culture media from each chamber every other day (day 1, 3, 5, and 7) and pool the aliquots from the same sample together (800 µl each).
- Quantify the cellular production of matrix metalloproteinase-1 (MMP1) and HA using an MMP1 ELISA Development kit and a hyaluronan competitive ELISA kit, respectively, following the manufacturers' procedure. Meanwhile, assay the production of soluble elastin precursor following the previously reported ELISA procedure.<sup>8</sup>
- Upon completion of the last vibration cycle at day 7, quickly remove the cellular constructs from the vibration chambers using sharp tweezers and briefly rinse them with cold phosphate buffered saline (PBS, 4 °C).
- For the live/dead staining, incubate the constructs with propidium iodide (1:2,000 in PBS) and Syto-13 (1:1,000 in PBS) simultaneously for 5 min at RT. Image the stained constructs with a multiphoton confocal microscope.
- Separately, snap-freeze the PBS-rinsed cellular constructs on dry ice and extract the total cellular RNA following a previously reported protocol for gene analysis.<sup>9</sup>
- Verify the quantity and quality of the extracted RNA using a UV-Vis spectrophotometer. RNA samples with A260/A280 and A260/A230 ratios of 1.8-2.2 are used for subsequent qPCR analysis.
- Reverse transcribe the RNA (500 ng/sample) into cDNA using a commercially available reverse transcription kit.
- Perform the PCR reaction on a real-time sequence detection system using a commercially available PCR master mix following the previously detailed procedure.<sup>8</sup>
- Analyze the qPCR results using commercial qPCR data analysis software. To ensure the reliability of the data analysis, multiple reference genes (YWHAZ, TBP, PPIA) are employed as internal controls, and the variance of specific primer efficiencies is taken into account.<sup>8</sup>

## Representative Results

The PCL scaffolds fabricated by electrospinning contain micron sized interstitial pores and randomly entangled fibers with an average diameter of 4.7 µm (**Figure 4A**). At a higher magnification, nanoscale grooves and pores are visible on individual fibers (**Figure 4B**). Coating of the scaffolds with fibronectin improves hydrophilicity and facilitates the initial cell adhesion/spreading on the PCL scaffold (unpublished observation).

Sinusoidal waveforms with desired frequency ( $f$ , 100-300 Hz) and voltage ( $V_{pp}$ : 0-0.125 V) are introduced to the speaker underneath each vibration chamber, and the air confined between the bottom of the silicone membrane and the paper cone of a mini-woofer is driven into oscillation. The air oscillation is delivered to the PCL scaffold with or without cells. LDV is used to analyze the vibration characteristics of the scaffold at a given  $f$  and  $V_{pp}$ , taking into account the refractive index of water (1.33).<sup>20</sup> **Figure 5** shows the normal displacement ( $w_0$ ) at the center of the PCL scaffold as a function of  $V_{pp}$  and  $f$ . The vibration frequencies are chosen to reflect fundamental human speaking frequencies.<sup>21</sup> There is a linear relationship between  $w_0$  and  $V_{pp}$  in the range of 0-0.125 V for all the frequencies tested. At a given  $V_{pp}$ ,  $w_0$  decreases as  $f$  increases from 100 to 300 Hz.

A specific vibration condition ( $f = 200$  Hz,  $V_{pp} = 0.1$  V) is selected for further analysis. The velocity profile as a function of time (**Figure 6A**) shows that the sinusoidal signal introduced to the speaker is captured by the PCL scaffold with high fidelity. The center of the PCL scaffold

oscillates longitudinally with a peak velocity of 52 mm/sec, a peak acceleration of 66 m/sec<sup>2</sup> (~6.7g) and a normal displacement of ~40 μm. The harmonic signals at 100, 300, 400 and 500 Hz are at least an order of magnitude lower than those at the fundamental frequency (200 Hz). However, if the Vpp value is too high (0.15 V), multiple harmonic peaks of comparable intensity to the fundamental frequency are detected (Figure 7). The vibration profile across the scaffold is created by monitoring the normal displacement from a total of 73 representative points on the radial directions of the PCL surface (Figure 3). The 3D colomap (Figure 8) demonstrates that the vibration detected on the surface of the membrane is axisymmetrical relative to the center and its resting positions. The normal displacement is found to decrease monotonically from the center to the edge where the membrane is secured.

MSCs cultured on PCL scaffolds are cultured under selected vibration conditions. Cells subjected to a 7-day OF stimulation maintain similar viability and proliferation properties as the static controls (Figure 9), confirming that the fibrous scaffolds were cytocompatible and the vibration applied resulted in no loss of viability. Cellular responses to vibratory stimulations are examined at the mRNA levels in terms of the expression of essential vocal fold ECM proteins, such as elastin (ELN), hyaluronan synthase-1 (HAS1), Col3A1 and MMP1 (Figure 10). The OF vibration leads to a 2.3 fold increase in ELN expression at day 7, relative to the static controls. The vibratory stimulations also increased Col3A1 expression moderately. It is noteworthy that the expression of major ECM remodeling enzymes, HAS1 and MMP1, is significantly augmented by the vibration signals. Specifically, the dynamic treatment resulted in a fold increase of ~1.7 and ~16.3 for HAS1 and MMP1 expression (both p < 0.05), respectively, over their static controls at day 7. Overall, the inductive effect of the vibrations on HAS1 and MMP1 was enhanced from day 3 to day 7.

To further substantiate the qPCR results, the cellular production of HA, soluble elastin and MMP1 is quantified by ELISA at the translational level (Figure 11). The dynamically cultured cells produce 4.2 ± 0.1 μg/mg (per dry scaffold weight) soluble elastin after 7 days of vibrations, whereas the static controls only accumulate 2.7 ± 0.2 μg/mg elastin. On average, 7-day OF vibrations result in 2.2- and 4.7-fold increase in HA and MMP1 secretion, relative to the corresponding static controls.

**Video 1:** A 3D simulation showing the assembly of a J2 bioreactor. The video was created by Autodesk 3ds Max Design (Courtesy of Congfei Xie).

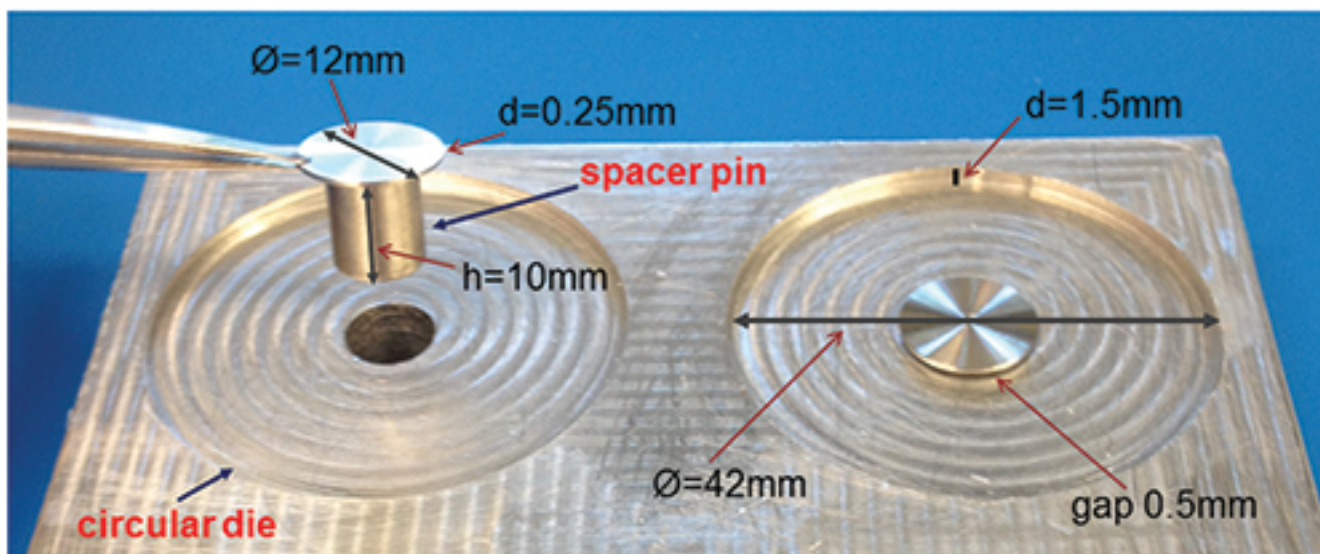


**Figure 1.** Photograph illustrating the dimension of the Al mold used for fabricating the silicone membrane with entrenched sleeve. Ø: diameter, d: thickness/depth, h: height. [Please click here to view a larger version of this figure.](#)

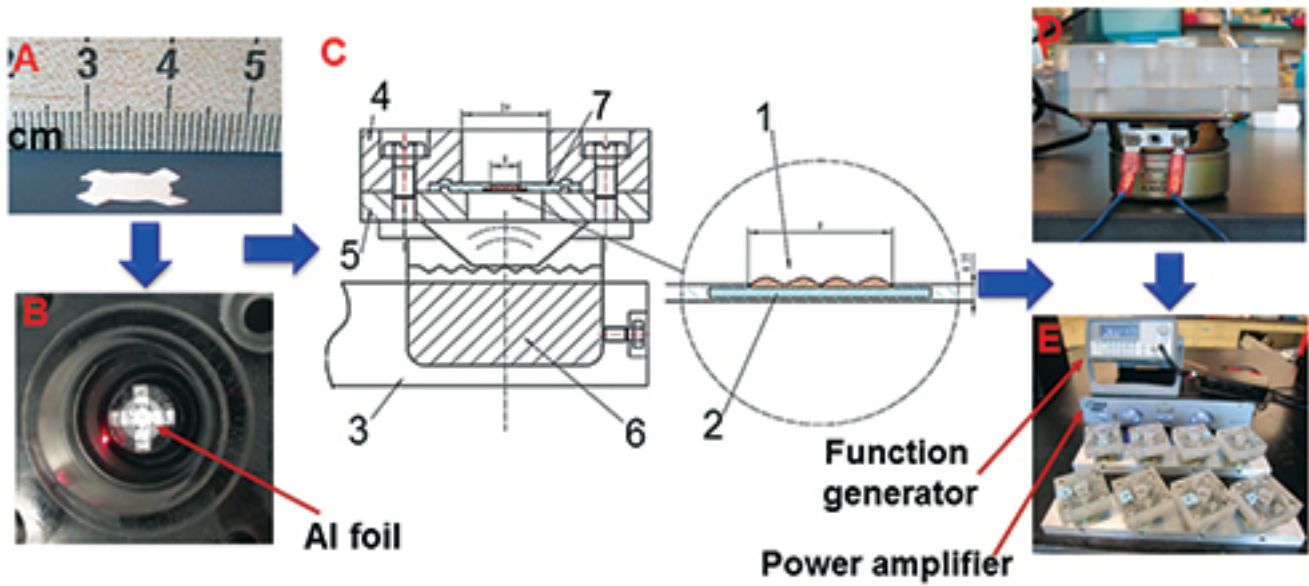


**Figure 2. Flowchart showing the bioreactor assembly.** (A) A photograph of a four-arm shaped PCL scaffold; (B) A photograph showing the PCL scaffold secured in the vibration chamber and the vibrometer laser focused on the bottom of the chamber; (C) A cross-sectional view of the vibration chamber. 1: PCL scaffold (red); 2: silicone membrane (cyan); 3: Al stationary bar; 4: top acrylic block; 5: bottom acrylic block; 6: mini-woofer; (D) side view of the vibration module; (E) A photograph showing the entire assembly. This figure has been modified from Tong *et al.*<sup>10</sup> Copyright 2013, Mary Ann Liebert, Inc. [Please click here to view a larger version of this figure.](#)

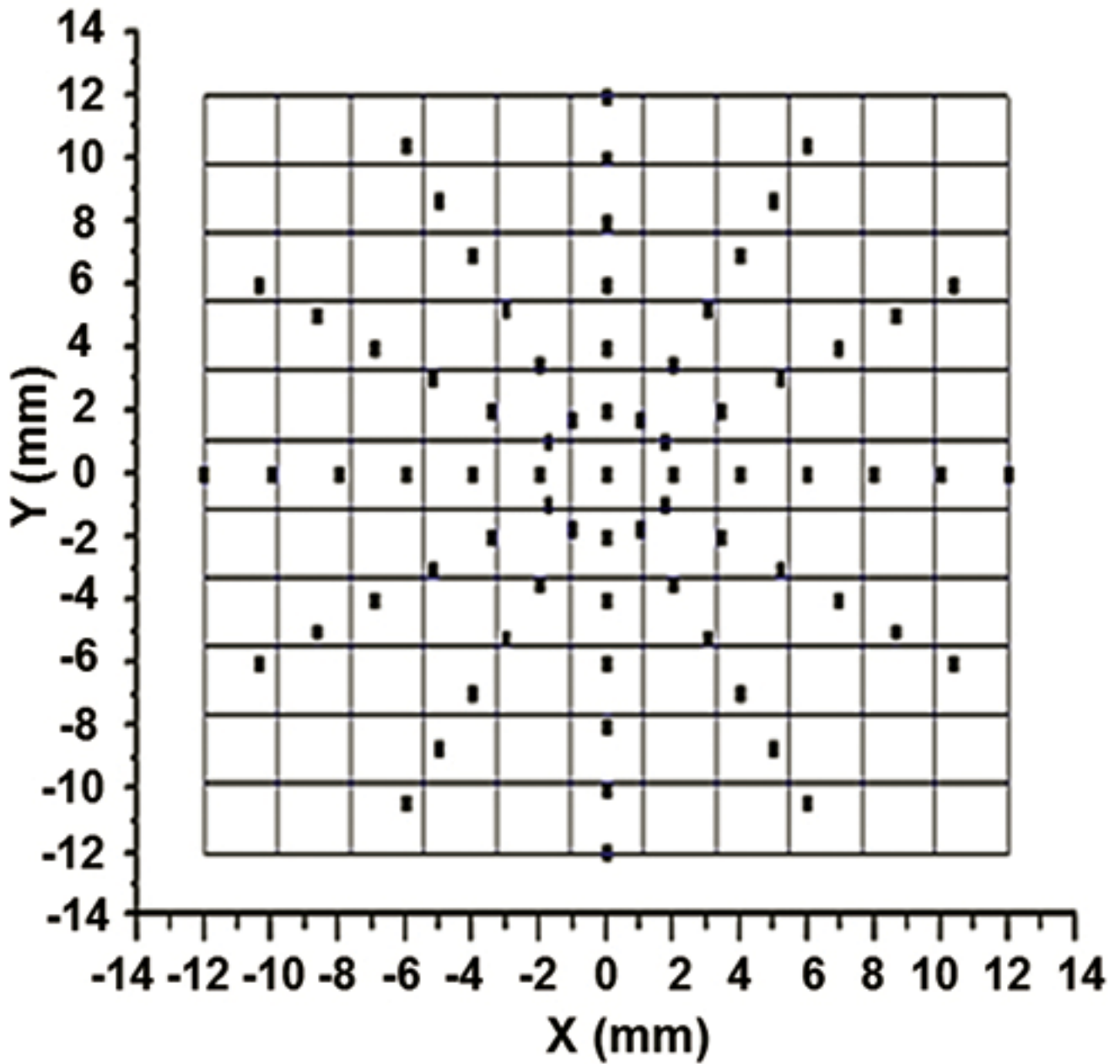
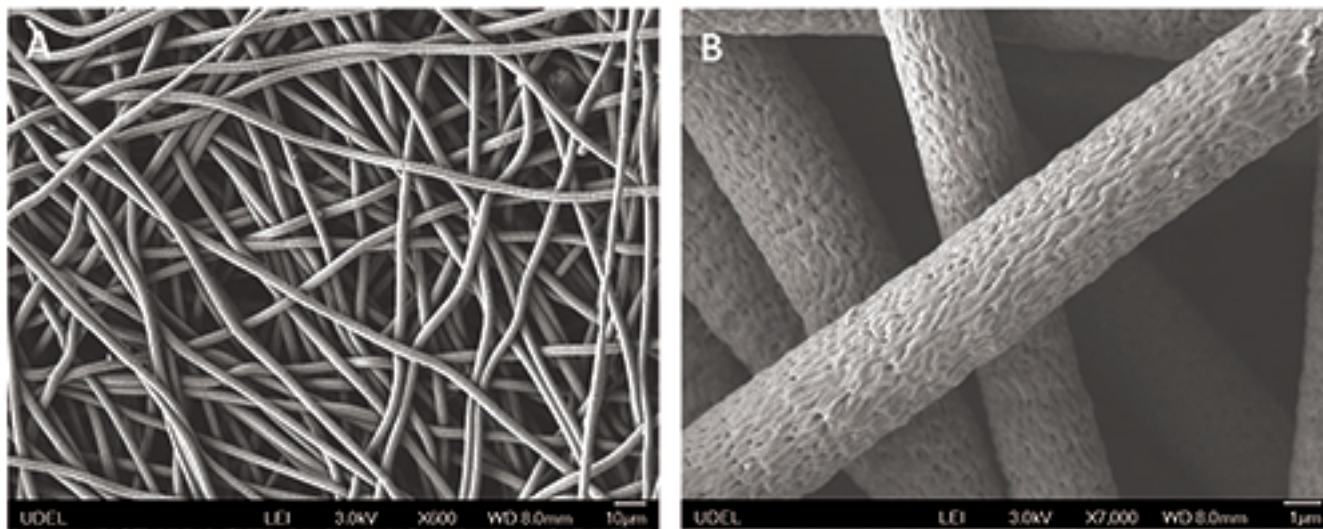


Figure 3. Illustration of radially marked silicone membrane for single point LDV measurements. This figure has been modified from Tong *et al.*<sup>10</sup> Copyright 2013, Mary Ann Liebert, Inc.



**Figure 4.** SEM images of PCL scaffolds at different magnifications. (A) 600X, (B) 7,000X. This figure has been modified from Tong *et al.*<sup>10</sup> Copyright 2013, Mary Ann Liebert, Inc. [Please click here to view a larger version of this figure.](#)

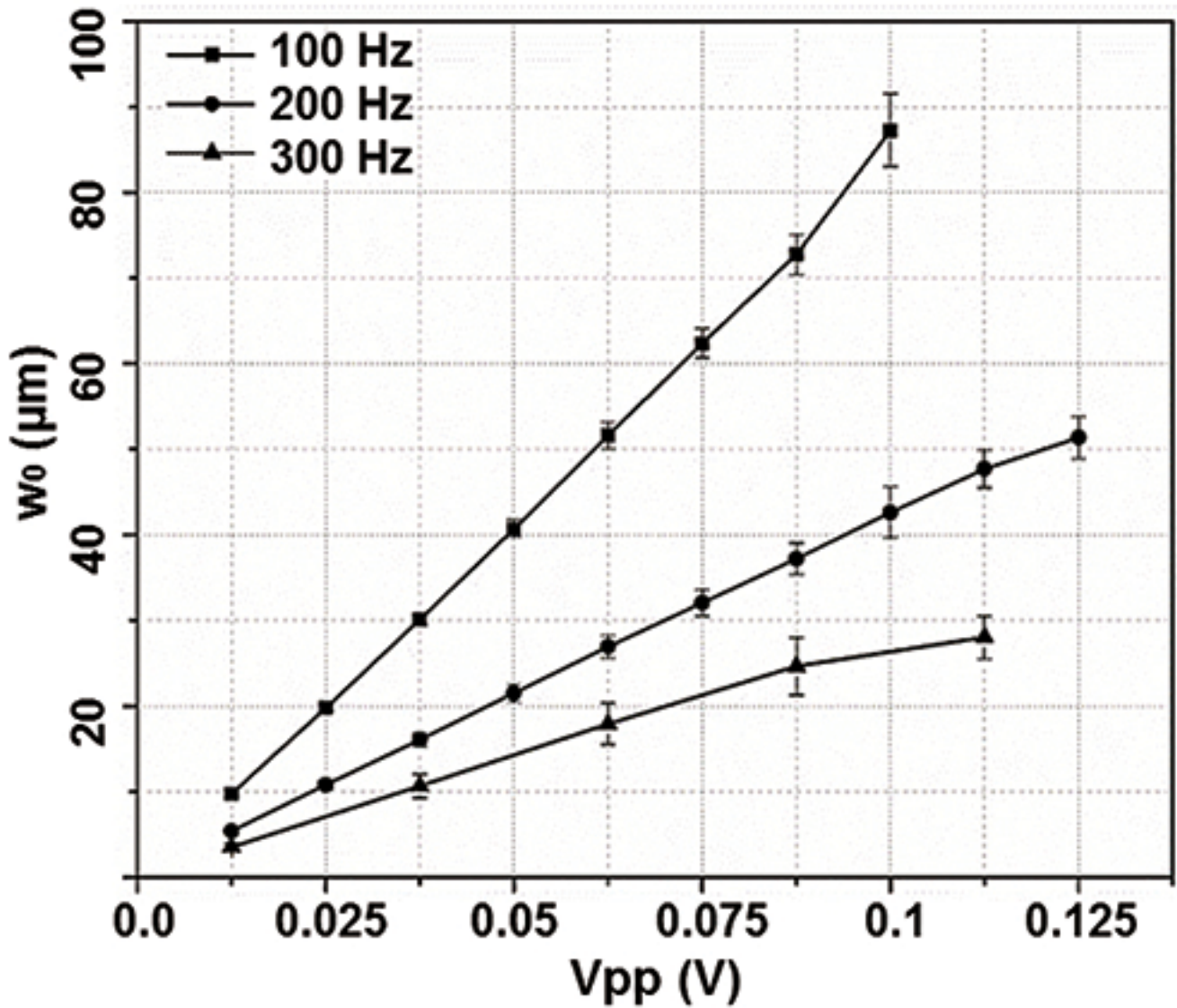
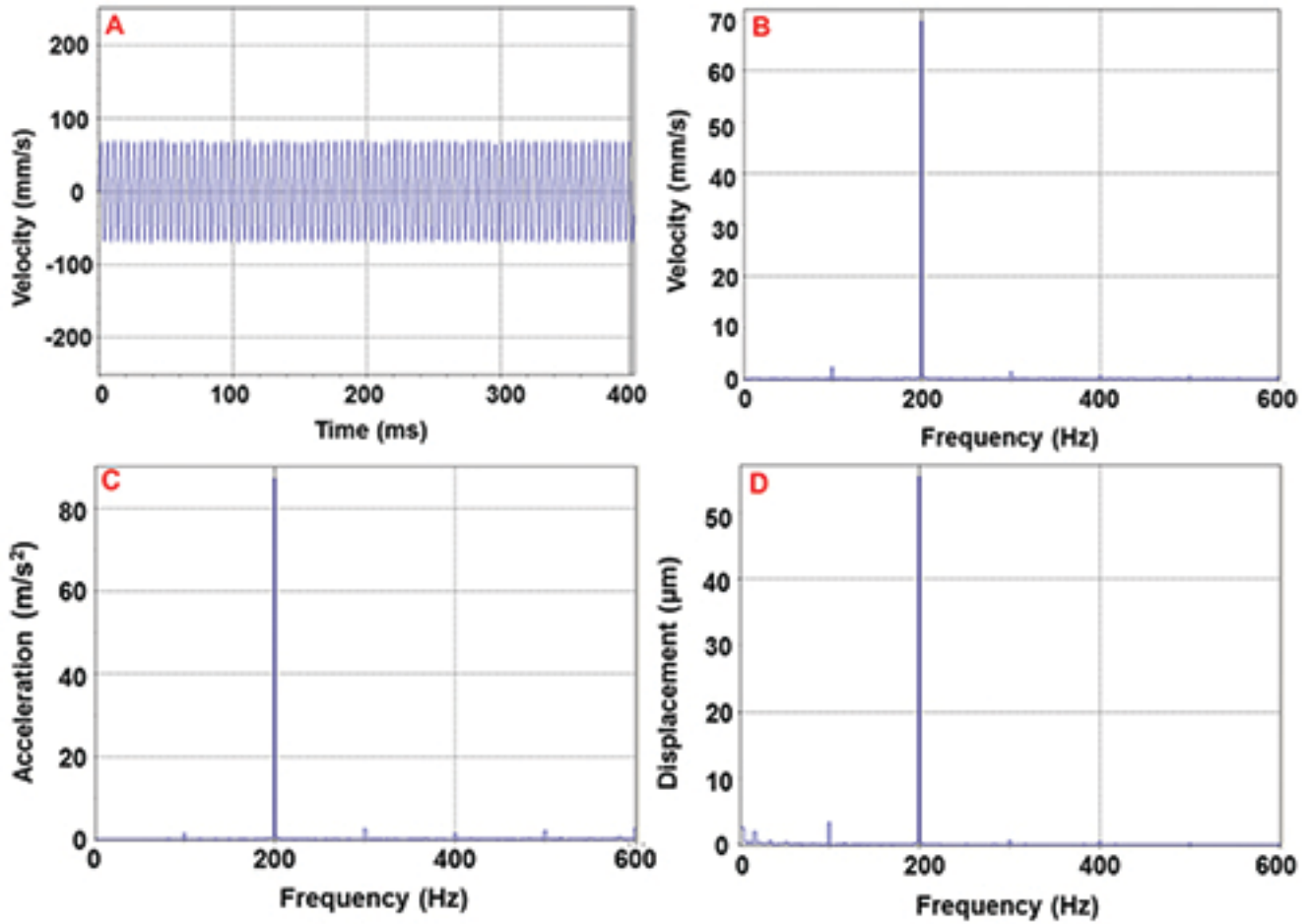


Figure 5. The normal displacement at the center of the silicone membrane ( $w_0$ ) as a function of the applied frequency (100, 200 and 300 Hz) and the driving voltage ( $V_{pp} = 0-0.125$  V). This figure has been modified from Tong *et al.*<sup>10</sup> Copyright 2013, Mary Ann Liebert, Inc.





**Figure 6. Vibration characteristics detected at the center of the silicone membrane with  $f = 200$  Hz and a  $V_{pp} = 0.1$  V. (A) Velocity profile as a function of time. (B) Velocity profile as a function of frequency. (C) Acceleration as a function of frequency. (D) Normal displacement ( $w_0$ ) as a function of frequency. This figure has been modified from Tong *et al.*<sup>10</sup>. Copyright 2013, Mary Ann Liebert, Inc. [Please click here to view a larger version of this figure.](#)**

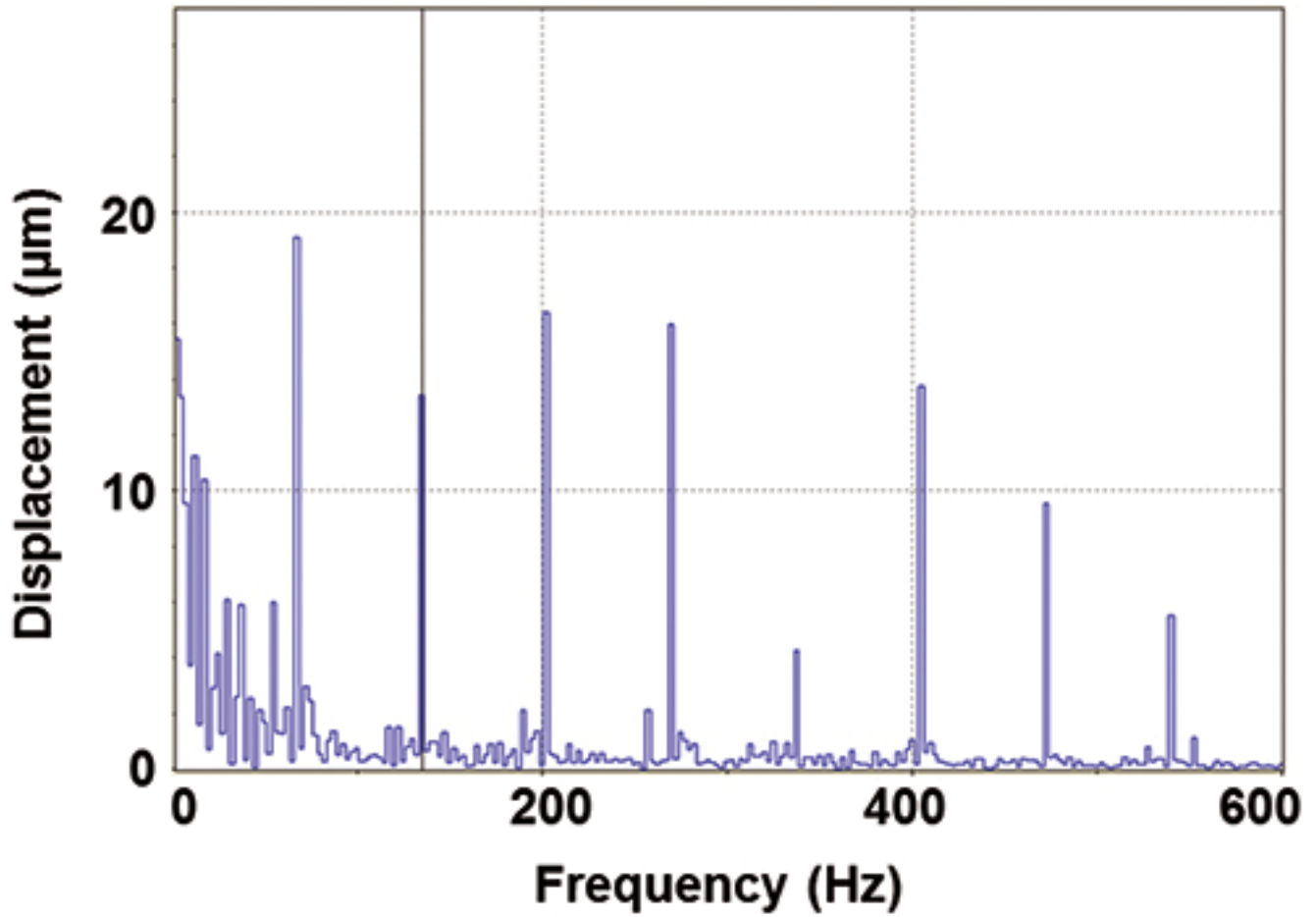


Figure 7. Normal displacement detected at the center of the membrane ( $w_0$ ) as a function of frequency when a 200 Hz sinusoidal wave is introduced to the mini-woofer at a  $V_{pp} = 0.15$  V.

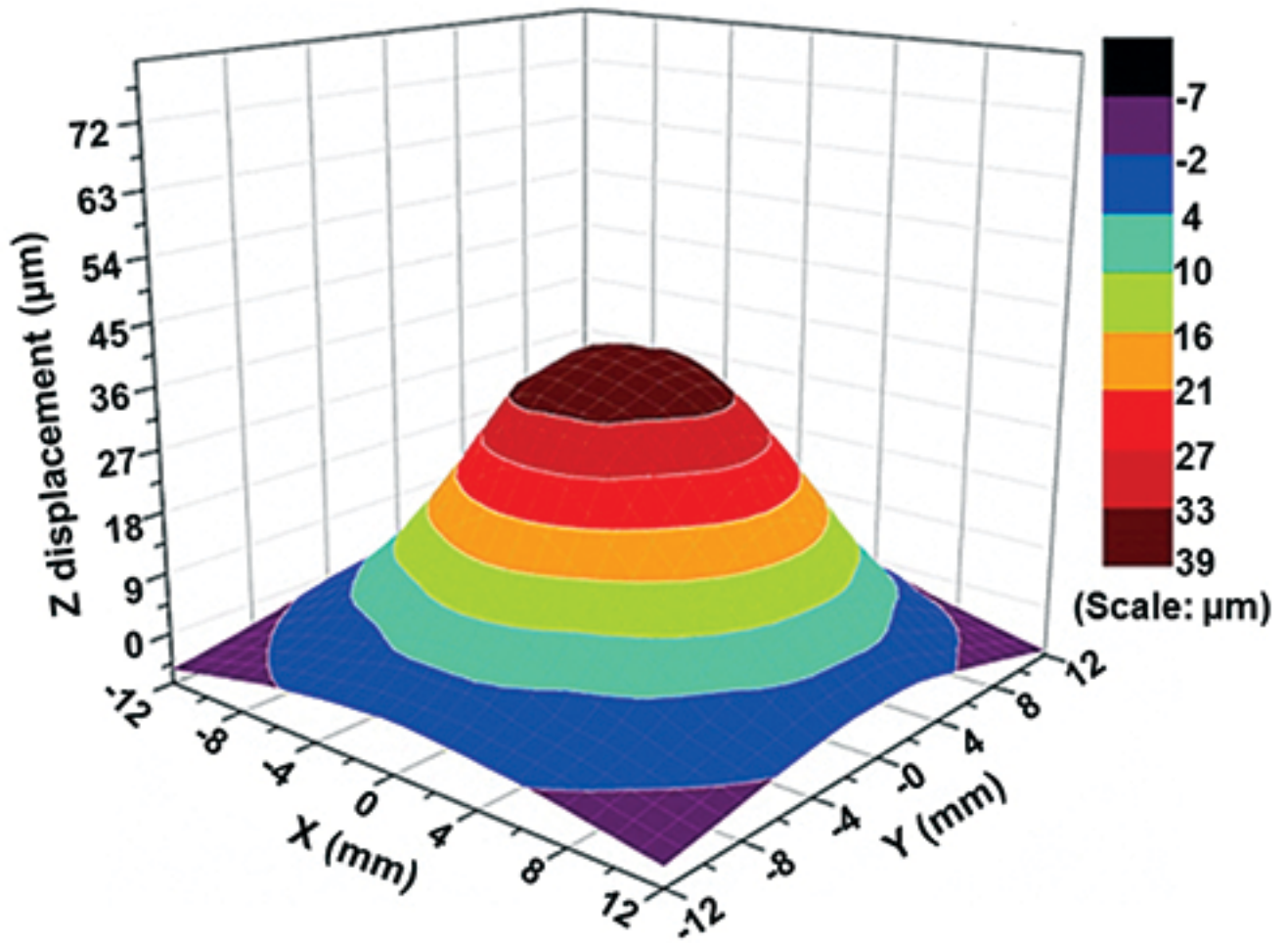
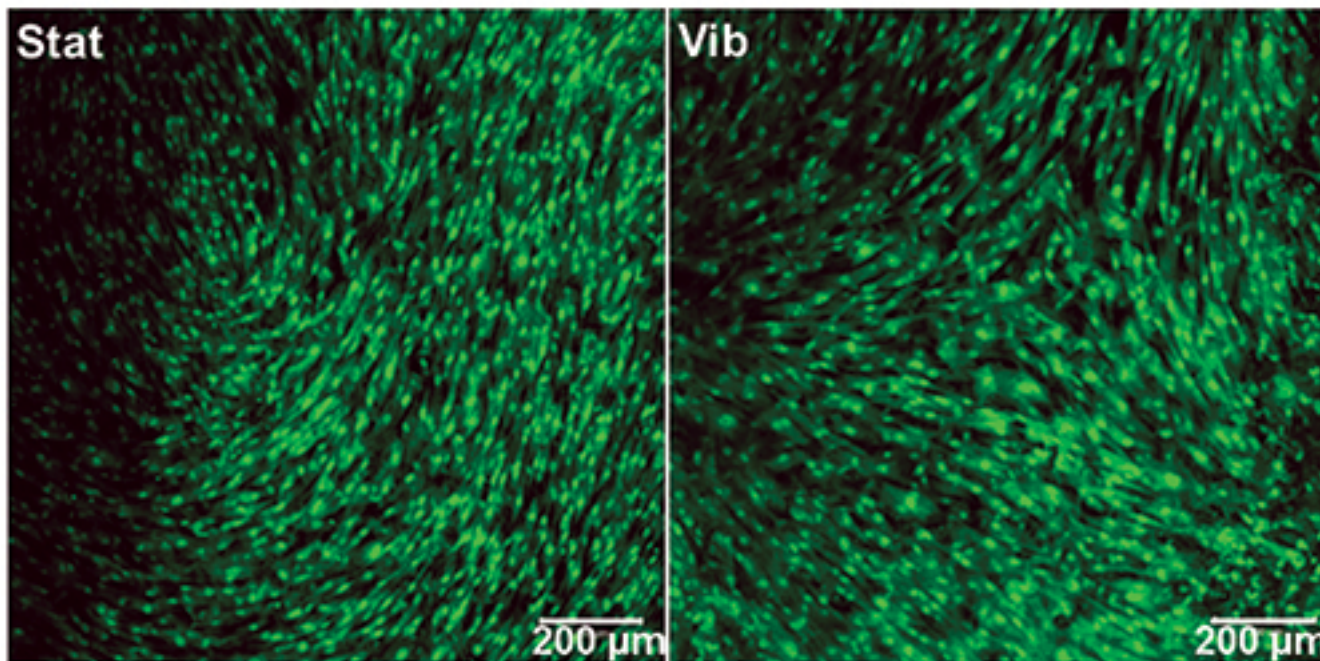
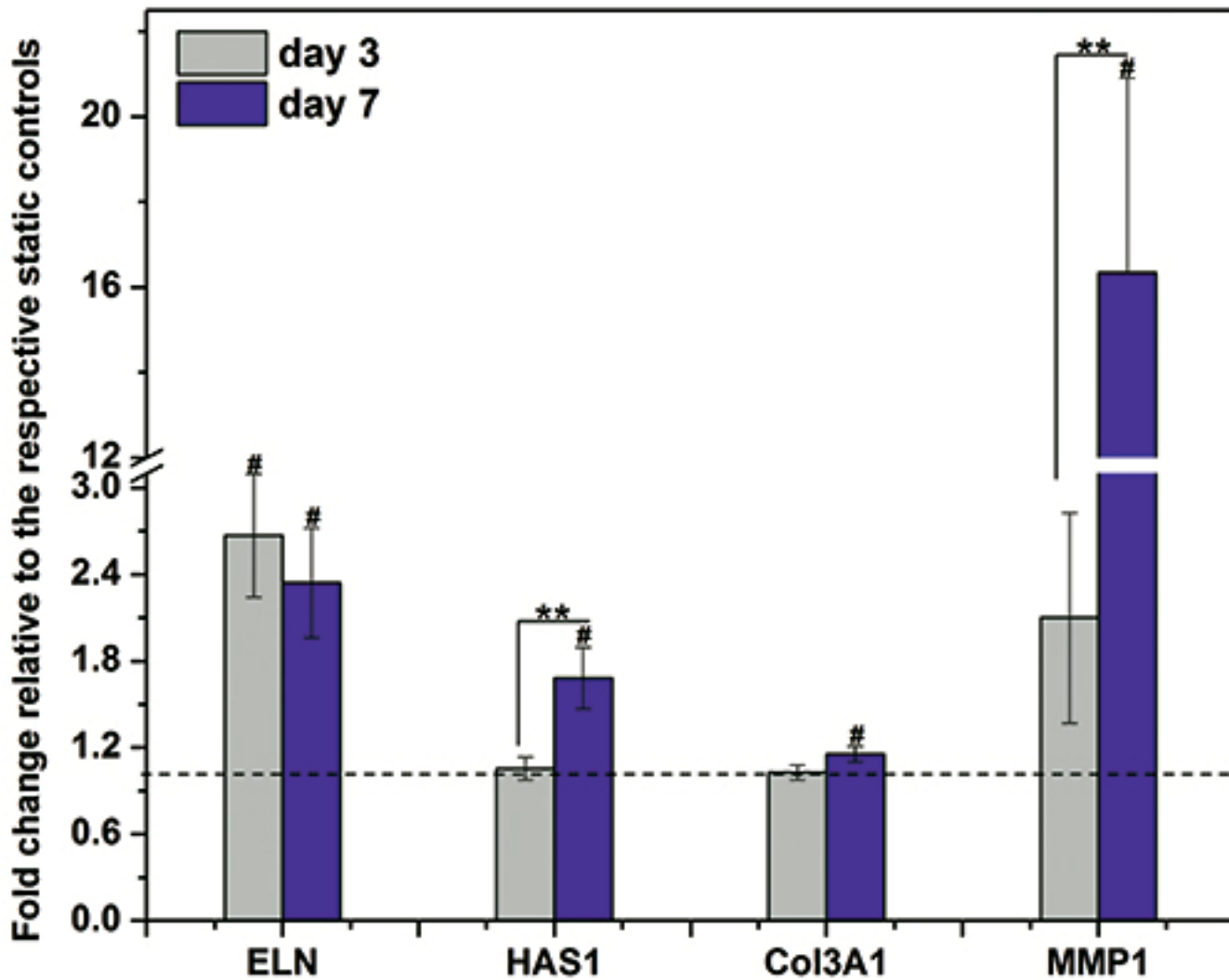


Figure 8. 3D colormap constructed by surface gridding using the normal displacement data collected from all locations marked on the PCL scaffold. This figure has been modified from Tong *et al.*<sup>10</sup> Copyright 2013, Mary Ann Liebert, Inc.



**Figure 9. Cell viability, visualized by live/dead staining, after 7 days of vibrations.** This figure has been modified from Tong *et al.*<sup>10</sup> Copyright 2013, Mary Ann Liebert, Inc. [Please click here to view a larger version of this figure.](#)



**Figure 10. Cellular responses to the vibratory stimulations in terms of the expression of vocal fold relevant, ECM genes.** The relative gene expression (fold change) is normalized to the respective static controls at day 3 and day 7 (dashed baseline). \*\*: significant difference ( $p < 0.05$ ) between day 3 and 7, #: significantly changed ( $p < 0.05$ ) relative to the baseline. Data represents mean  $\pm$  standard error of the mean (S.E.M, n=4). Two-tailed student's *t*-test is used for statistical analysis, with  $p < 0.05$  being considered as significantly difference (same as below). This figure has been modified from Tong *et al.*<sup>10</sup> Copyright 2013, Mary Ann Liebert, Inc.

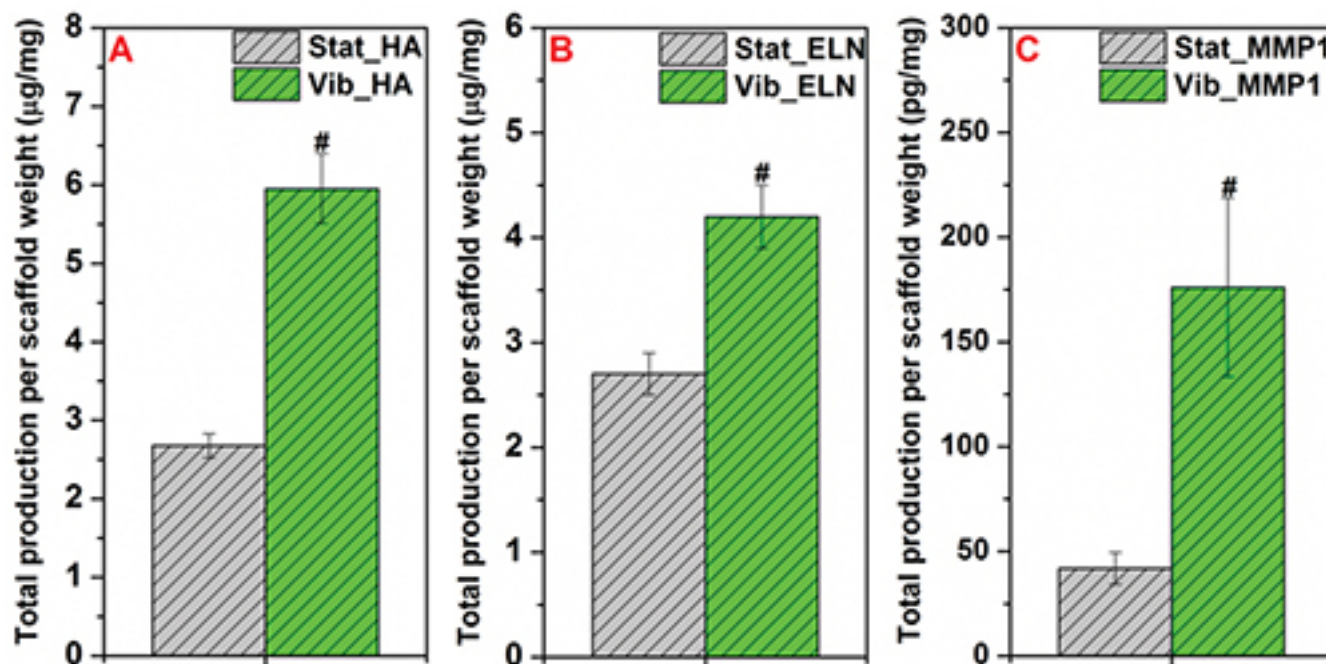


**Figure 11. Biochemical quantification of HA (A), soluble ELN (B) and MMP1 (C) produced by MSCs cultured on the PCL scaffold under Stat and Vib conditions for 7 days.** Total amount of ECM molecules per dry scaffold weight (mg) is represented as mean  $\pm$  S.E.M, n = 4 from the representative trial. #: significantly enhanced ( $p < 0.05$ ) compared to the Stat controls. This figure has been modified from Tong *et al.*<sup>10</sup> Copyright 2013, Mary Ann Liebert, Inc.

## Discussion

Successful engineering of functional vocal fold tissues *in vitro* requires the recreation of a vocal fold-like microenvironment to mediate the behaviors of multipotent cells. It is generally accepted that tissue or organ structures reflect the functions they are required to perform.<sup>22</sup> For vocal fold tissues, the high frequency vibrations that occur during phonation are proposed to be important for tissue maturation. In our study, PCL scaffolds are used to provide a ligament-like structural support while the vocal fold bioreactor is designed to introduce physiologically relevant mechanical signals to the cultured MSCs. The bioreactor described here (J2) creates the vibration electromagnetically through individual speakers and transfers the energy aerodynamically to the cultured cells. Compared to our previous design,<sup>18</sup> the current system moves the source of vibrational stimulation directly below each sample well, allowing for a more efficient energy conversion. As a result, a significantly larger normal displacement and a higher acceleration are achieved using the current system. The modular design also minimizes system variations and mechanical perturbation across different vibration chambers.

Our design relies on a silicone membrane to deliver the vibration signals. It is therefore important to maintain the membrane integrity and homogeneity. After the precursor solution is poured into the aluminum mold, it is desirable to remove the excess liquid by dragging a glass slide across the mold surface. Consistent membranes without any entrapped air bubbles can be produced by lowering curing temperature while increasing curing time. Additionally, a 70% ethanol solution can be used to temporarily swell the membrane at the aluminum interface to allow easy removal of the cured silicone. To accommodate the cellular constructs for 3D dynamic culture, a centrally positioned thin groove is molded into the silicone membrane, such that the PCL scaffolds can be peripherally anchored in the vibration chamber. The geometry of the groove is adjustable; thus the shape of the cellular construct can be tuned accordingly to better mimic the geometry of native vocal folds.<sup>23</sup> If the PCL scaffold is not tightly secured in the silicone membrane, the LDV signals detected at the PCL and at the outer region on the silicone membrane will not overlap perfectly. When assembling the bioreactor, it is critical that all components are secured and tightened to the same degree so as to avoid undesirable motions and to minimize chamber to chamber variations.

To validate the utility of the bioreactor, MSCs are cultivated on PCL scaffolds and are subjected to intermittent (OF) vibrations for 7 days. The OF vibrations over a period of several hours per day are employed to reproduce the speaking conditions of heavy voice users, e.g., professional singers and teachers.<sup>23</sup> Unlike previously reported vocal fold bioreactors, ours do not cause any detrimental effect or physiological trauma to the cells.

The 200-Hz vibrations are found to differentially regulate cellular production of important ECM components. Elastin is a crucial structural protein that is found throughout the vocal fold LP, and imparts resilience and elasticity.<sup>24</sup> Interstitial amorphous components, such as HA, contribute to the maintenance of proper tissue viscoelasticity and the prevention of scar formation.<sup>25,26</sup> MSCs subjected to the 7-day OF treatment produce a significantly higher amount of elastin than the statically cultured counterparts. HA biosynthesis is also sensitive to the vibrations, as confirmed by qPCR results on HAS1 and ELISA results on HA. These findings suggest that the vibrational stimulation enabled by the bioreactor is conducive to the production of anti-scarring molecules.

Balanced ECM turnover relies on concurrent matrix deposition and degradation.<sup>27</sup> Type III collagen is the major reticular collagen fiber found in vocal folds, providing the tissue with load-bearing properties.<sup>28</sup> The 7-day vibrations applied herein enhance the gene expression of *Co3A1*,

but at a magnitude much lower than that of elastin. Therefore, the applied vibrations differentially regulate cellular machinery involved in the synthesis of collagen III and elastin. Interestingly, MMP1, one of the major MMPs involved in matrix degradation and tissue remodeling<sup>27</sup>, is highly sensitive to the vibratory cues. These results agree well with previous reports on vibration-induced MMP1 upregulation by cells entrapped in a HA matrix.<sup>29</sup> Overall, the vibratory stimulations generated by the vocal fold bioreactor profoundly mediate MSC functions by promoting the homeostasis of vocal fold-like matrices.

Overall, the novel vocal fold bioreactor presented here is modular and user-friendly, allowing dynamic cell culture to be performed in a reproducible fashion. However, several limitations exist in the current design. First, the vibration amplitude, although improved from the J1 version, is still small compared to the vocal fold tissue. Second, our bioreactor does not simulate the bilateral collision of vocal folds during normal phonation. Third, our fibrous PCL scaffold does not reflect the tissue anisotropy. Future work is dedicated to improving the design to better mimic the native phonation conditions. Meanwhile, optimal regimes for 3D dynamic culture will be explored for the successful functional vocal fold assembly *in vitro*.

## Disclosures

No competing financial interests exist.

## Acknowledgements

We thank Dr. Jeffrey Caplan for his training and advice on confocal imaging. We also thank the Keck Electron Microscopy Lab and Dr. Chaoying Ni for SEM assistance. This work is funded by National Institutes of Health (NIDCD, R01DC008965 and R01DC011377). ABZ acknowledges NSF Integrative Graduate Education & Research Traineeship (IGERT) program for funding.

## References

1. Titze, I. R. Mechanical-Stress in Phonation. *J. Voice*. **8**, 99-105 (1994).
2. Titze, I. R. On the Relation Between Subglottal Pressure and Fundamental-Frequency in Phonation. *J. Acoust. Soc. Am.* **85**, 901-906 (1989).
3. Gray, S. D. Cellular physiology of the vocal folds. *Otolaryngol. Clin. N. Am.* **33**, 679-698 (2000).
4. Thibeault, S. L., Gray, S. D., Bless, D. M., Chan, R. W., & Ford, C. N. Histologic and rheologic characterization of vocal fold scarring. *J. Voice*. **16**, 96-104 (2002).
5. Hansen, J. K., & Thibeault, S. L. Current understanding and review of the literature: Vocal fold scarring. *J. Voice*. **20**, 110-120 (2006).
6. Pittenger, M. F. *et al.* Multilineage potential of adult human mesenchymal stem cells. *Science*. **284**, 143-147 (1999).
7. Hanson, S. E. *et al.* Characterization of Mesenchymal Stem Cells From Human Vocal Fold Fibroblasts. *Laryngoscope*. **120**, 546-551, (2010).
8. Tong, Z., Duncan, R. L., & Jia, X. Modulating the behaviors of mesenchymal stem cells via the combination of high-frequency vibratory stimulations and fibrous scaffolds. *Tissue Eng. Part A*. **19**, 1862-1878 (2013).
9. Tong, Z., Sant, S., Khademhosseini, A., & Jia, X. Controlling the Fibroblastic Differentiation of Mesenchymal Stem Cells Via the Combination of Fibrous Scaffolds and Connective Tissue Growth Factor. *Tissue Eng. Part A*. **17**, 2773-2785 (2011).
10. Jones, D. L., & Wagers, A. J. No place like home: anatomy and function of the stem cell niche. *Nat. Rev. Mol. Cell Biol.* **9**, 11-21 (2008).
11. Wang, J. H., & Thampatty, B. P. Mechanobiology of Adult and Stem Cells. *Int. Rev. of Cell Mol. Biol.* **271**, 301-346 (2008).
12. Doroski, D. M., Levenston, M. E., & Temenoff, J. S. Cyclic tensile culture promotes fibroblastic differentiation of marrow stromal cells encapsulated in poly (ethylene glycol)-based hydrogels. *Tissue Eng. Part A*. **16**, 3457-3466 (2010).
13. Kim, B. S., Nikolovski, J., Bonadio, J., & Mooney, D. J. Cyclic mechanical strain regulates the development of engineered smooth muscle tissue. *Nat. Biotechnol.* **17**, 979-983 (1999).
14. Webb, K. *et al.* Cyclic strain increases fibroblast proliferation, matrix accumulation, and elastic modulus of fibroblast-seeded polyurethane constructs. *J. Biomech.* **39**, 1136-1144 (2006).
15. Kim, Y. J., Sah, R. L. Y., Grodzinsky, A. J., Plaas, A. H. K., & Sandy, J. D. Mechanical Regulation of Cartilage Biosynthetic Behavior - Physical Stimuli. *Arch. Biochem. Biophys.* **311**, 1-12 (1994).
16. Titze, I. R. *et al.* Design and validation of a bioreactor for engineering vocal fold tissues under combined tensile and vibrational stresses. *J. Biomech.* **37**, 1521-1529 (2004).
17. Kutty, J. K., & Webb, K. Vibration stimulates vocal mucosa-like matrix expression by hydrogel-encapsulated fibroblasts. *J. Tissue Eng. Regen. Med.* **4**, 62-72 (2010).
18. Farran, A. J. E. *et al.* Design and Characterization of a Dynamic Vibrational Culture System. *J. Tissue Eng. Regen. Med.* (2011).
19. Reneker, D. H., & Yarin, A. L. Electrospinning jets and polymer nanofibers. *Polymer*. **49**, 2387-2425 (2008).
20. Wang, Y., Theobald, P., Tyrer, J., & Lepper, P. The application of scanning vibrometer in mapping ultrasound fields. *J. Phys.: Conf. Ser.* **1**, 167-173 (2004).
21. Brown, W. S., Morris, R. J., Hollien, H., & Howell, E. Speaking Fundamental-Frequency Characteristics as a Function of Age and Professional Singing. *J. Voice*. **5**, 310-315 (1991).
22. Ingber, D. E. Cellular mechanotransduction: putting all the pieces together again. *Faseb J.* **20**, 811-827 (2006).
23. Titze, I. R. *et al.* Design and validation of a bioreactor for engineering vocal fold tissues under combined tensile and vibrational stresses. *J. Biomech.* **37**, 1521-1529 (2004).
24. Moore, J., & Thibeault, S. Insights Into the Role of Elastin in Vocal Fold Health and Disease. *J. Voice*. **26**, 269-275 (2012).
25. Thibeault, S. L., Bless, D. M., & Gray, S. D. Interstitial protein alterations in rabbit vocal fold with scar. *J. Voice*. **17**, 377-383 (2003).
26. Branski, R. C., Verdolini, K., Sandulache, V., Rosen, C. A., & Hebda, P. A. Vocal fold wound healing: A review for clinicians. *J. Voice*. **20**, 432-442 (2006).
27. Clark, I. A., Swingler, T. E., Sampieri, C. L., & Edwards, D. R. The regulation of matrix metalloproteinases and their inhibitors. *Int. J. Biochem. Cell B.* **40**, 1362-1378 (2008).

28. Silver, F. H., Horvath, I., & Foran, D. J. Viscoelasticity of the vessel wall: The role of collagen and elastic fibers. *Crit. Rev. Biomed. Eng.* **29**, 279-301 (2001).
29. Kutty, J. K., & Webb, K. Tissue Engineering Therapies for the Vocal Fold Lamina Propria. *Tissue Eng. Part B: Rev.* **15**, 249-262 (2009).